

# Two-dimensional black holes in accelerated frames: Spacetime structure

R. Balbinot

*Dipartimento di Fisica dell'Università di Bologna and INFN sezione di Bologna,  
Via Irnerio 46, 40126 Bologna, Italy  
balbinot@bologna.infn.it*

A. Fabbri

*SISSA-ISAS and INFN sezione di Trieste,  
Via Beirut 2-4, 34014 Trieste, Italy  
fabbri@gandalf.sissa.it*

## Abstract

Analytical extensions and resulting Penrose diagrams are given for the solutions of a simple 2d dilaton gravity theory describing black holes which are static as viewed by asymptotically accelerated observers.

## 1. Introduction

Two-dimensional theories of gravity represent very simple schemes used nowadays to investigate issues related to black holes evaporation.

One of the most popular models, the RST [1], has the advantage of being exactly solvable; it describes in a closed analytical form the semiclassical physics of an evaporating black hole (i.e. formation, evaporation and backreaction).

In a previous paper [2] it has been shown that there exists a one parameter family of classical theories all leading to the RST action at the semiclassical level. These theories are described by the action

$$S_n = \frac{1}{2\pi} \int d^2x \sqrt{-g} [e^{-\frac{2}{n}\phi} (R + \frac{4}{n}(\nabla\phi)^2) + 4\lambda^2 e^{-2\phi}], \quad (1.1)$$

where  $R$  is the scalar curvature associated to the two-dimensional metric tensor  $g_{ab}$ ,  $\phi$  is the dilaton field. In the case  $n = 1$ , eq. (1.1) is the usual CGHS action [3].

The geometries which extremize  $S_n$  have been shown to have typically a black hole structure with curvature singularities, horizons and regions where  $R$  vanishes.

However, their most striking feature is that the natural frame in which the metric is static is not ‘asymptotically’ minkowskian but Rindler like.<sup>1</sup> Depending on the value of the parameter  $n$ , the ‘asymptotic region’ where the spacetime becomes flat ( $R \rightarrow 0$ ) corresponds either to true infinity (in the sense that geodesic observers take an infinite amount of their proper time to reach this region) or just to the location of another horizon (besides the black hole one), the acceleration horizon, which inertial observers can cross in a finite proper time.

All the solutions possess a Killing vector whose norm vanishes on one or more horizons. The analytical extension beyond these horizons reveals a very rich and interesting spacetime structure which is the object of the present paper.<sup>2</sup>

## 2. The theory and its solutions

For the theory described by the action  $S_n$ , the equations of motion are

$$g_{\mu\nu} \left[ \frac{4}{n} \left( -\frac{1}{2} + \frac{1}{n} \right) (\nabla\phi)^2 - \frac{2}{n} \nabla^2\phi - 2\lambda^2 e^{\frac{2-2n}{n}\phi} \right] + \frac{4}{n} \left( 1 - \frac{1}{n} \right) \partial_\mu\phi \partial_\nu\phi \quad (2.1)$$
$$+ \frac{2}{n} \nabla_\mu \partial_\nu \phi = 0 ,$$

---

<sup>1</sup> This seems a common feature of 2d black holes, see for example [4].

<sup>2</sup> The spacetime structure of other models of 2d black holes are discussed in Refs [5] and [6].

$$\frac{R}{n} - \frac{4}{n^2}(\nabla\phi)^2 + \frac{4}{n}\nabla^2\phi + 4\lambda^2 e^{\frac{2-2n}{n}\phi} = 0. \quad (2.2)$$

The solution of these equations is easily derived in the conformal gauge  $g_{\pm\pm} = 0$ ,  $g_{+-} = -\frac{1}{2}e^{2\rho}$ . Eqs (2.1) and (2.2) then become

$$-\frac{4}{n^2}\partial_+\phi\partial_-\phi + \frac{2}{n}\partial_+\partial_-\phi - \lambda^2 e^{\frac{2-2n}{n}\phi+2\rho} = 0, \quad (2.3)$$

$$\frac{2}{n}\partial_+\partial_-\rho + \frac{4}{n^2}\partial_+\phi\partial_-\phi - \frac{4}{n}\partial_+\partial_-\phi + \lambda^2 e^{\frac{2-2n}{n}\phi+2\rho} = 0. \quad (2.4)$$

These equations have to be supplemented by the constraints

$$e^{-\frac{2}{n}\phi} \left[ \frac{4}{n} \left(1 - \frac{1}{n}\right) \partial_{\pm}\phi\partial_{\pm}\phi + \frac{2}{n}\partial_{\pm}^2\phi - \frac{4}{n}\partial_{\pm}\rho\partial_{\pm}\phi \right] = 0. \quad (2.5)$$

From (2.3) and (2.4) it follows that

$$\frac{2}{n}\partial_+\partial_-(\rho - \phi) = 0, \quad (2.6)$$

which implies

$$\rho = \phi + f_+(x^+) + f_-(x^-). \quad (2.7)$$

One can now perform a coordinate transformation  $x^{\pm} \rightarrow x'^{\pm} = F_{\pm}(x^{\pm})$  which preserves the conformal gauge and for which  $\rho = \phi$ .

In this ‘Kruskal’ gauge the remaining field equation takes the form

$$\partial_+\partial_-(e^{-\frac{2}{n}\phi}) = -\lambda^2 \quad (2.8)$$

and the constraints

$$\partial_{\pm}^2(e^{-\frac{2}{n}\phi}) = 0. \quad (2.9)$$

The general solution can therefore be given as

$$e^{-\frac{2}{n}\phi} = e^{-\frac{2}{n}\rho} = -\lambda^2 x^+ x^- + \frac{M}{\lambda} \quad (2.10)$$

where  $M$  is a constant.

As shown in [2] the solution (2.10) describes a black hole and the constant  $M$  can be interpreted as the mass of the black hole. The line element of the solution is

$$ds^2 = -\frac{1}{\left(\frac{M}{\lambda} - \lambda^2 x^+ x^-\right)^n} dx^+ dx^- \quad (2.11)$$

and the scalar curvature  $R$  is

$$R = 8e^{-2\rho}\partial_+\partial_-\rho = 4M\lambda n \left[ \frac{M}{\lambda} - \lambda^2 x^+ x^- \right]^{n-2}. \quad (2.12)$$

For later purposes it is convenient to recast the line element (2.11) in a chiral form

$$ds^2 = -h(v, x)dv^2 + 2dvdx. \quad (2.13)$$

To this end we perform the following coordinate transformation

$$x^+ = V, \quad x^+x^- = \frac{r}{\lambda} \quad (2.14)$$

followed by

$$V = \frac{1}{\lambda}e^{\lambda v}, \quad x = \frac{(\frac{M}{\lambda} - \lambda r)^{1-n}}{2(1-n)\lambda} \quad (2.15)$$

which yields the desired chiral form of the line element, namely

$$ds^2 = -\{2(1-n)\lambda x - \frac{M}{\lambda}[2(1-n)\lambda x]^{\frac{n}{n-1}}\}dv^2 + 2dvdx. \quad (2.16)$$

One should note that  $x < 0$  for  $n > 1$  and  $x > 0$  for  $n < 1$ .

With this choice of coordinates  $v$  labels ingoing null lines and  $x$  is an appropriately normalized affine parameter on them.

As  $h$  in (2.16) does not depend on  $v$ , this metric has a Killing field  $\partial_v$  with Killing trajectories  $x = \text{const}$ . The function  $h$  measures the norm of this Killing vector.

In particular, the spacetime is stationary if the Killing field is timelike ( $h > 0$ ) or homogeneous if the field is spacelike ( $h < 0$ ). A zero of  $h$  corresponds to a Killing horizon.

From eq. (2.16) our metric function  $h$  is therefore

$$h(x) = 2(1-n)\lambda x - \frac{M}{\lambda}[2(1-n)\lambda x]^{\frac{n}{n-1}} \quad (2.17)$$

and for later use we give also the derivatives of  $h$

$$h'(x) = 2(1-n)\lambda \left\{ 1 - \frac{M}{\lambda} \left( \frac{n}{n-1} \right) [2(1-n)\lambda x]^{\frac{1}{n-1}} \right\} \quad (2.18)$$

and

$$h''(x) = -4M\lambda n [2(1-n)\lambda x]^{\frac{2-n}{n-1}}. \quad (2.19)$$

Finally in these chiral coordinates the scalar curvature  $R$  is simply

$$R = -h''(x) = 4M\lambda n [2(1-n)\lambda x]^{\frac{2-n}{n-1}} \quad (2.20)$$

and the dilaton field gives the coupling

$$e^{\frac{2}{n}\phi} = [2(1-n)\lambda x]^{\frac{1}{n-1}} \quad (2.21)$$

and the cosmological constant term

$$e^{-2\phi} = [2(1-n)\lambda x]^{\frac{n}{1-n}}. \quad (2.22)$$

### 3. Space-time structure - The method

In order to analyse the spacetime structure of our solutions and construct the corresponding maximally extended Penrose diagrams, we apply the method developed by Klösch and Strobl in [6] (to which we refer for the details).

This method consists in a set of basic rules which allows, starting from ‘building blocks’, to construct the maximally extended Penrose diagram corresponding to any metric function  $h$  in eq. (2.13) which depends on  $x$  only (as in our case).

The recipe is the following (for the case that the zeros of  $h(x)$  are of odd order):

a) the number of zeros of  $h$  determines the number of sectors and their ‘orientation’ in a fundamental building block.  $h > 0$  corresponds to a stationary sector,  $h < 0$  to an homogeneous one. For  $n$  zeros of  $h$  there are therefore  $n+1$  sectors. A zero of  $h$  corresponds to a Killing horizon which separates a stationary from an homogeneous sector.

b) The end sector of the building block is a triangle if

$$f(x) = \int^x \frac{du}{h(u)} \quad (3.1)$$

remains finite at the boundary; it is a square if  $f(x)$  diverges.

c) Choose any sector and establish the symmetry axis, running diagonally through the sector, transversal to the Killing line. The ‘flip’ symmetry

$$x \rightarrow x, \quad v \rightarrow -v + 2f(x) \quad (3.2)$$

amounts to a time reversal symmetry  $t \rightarrow -t$  in the Schwarzschild gauge

$$ds^2 = -h(x)dt^2 + \frac{dx^2}{h(x)}. \quad (3.3)$$

This symmetry corresponds to a reflection symmetry of the sector with respect to the above symmetry axis. Reflect the whole block at this symmetry axis and identify the corresponding sector.

d) Repeat this procedure for all sectors until one comes to an end or ad infinitum.

e) If, after surrounding a vertex point, the sectors overlap, identify the overlapping sectors such as to make a single sheet around this vertex point.

A boundary of the resulting diagram is null complete iff  $x \rightarrow \pm\infty$  there. A boundary point is complete with respect to all other geodesics iff

$$l(x) = \int^x \frac{du}{\sqrt{|c-h(u)|}} \quad (3.4)$$

diverges there ( $c$  is a constant).

With these simple rules we proceed to the construction of the Penrose diagrams for the space-times of our theory. The discussion will be divided in paragraphs, each corresponding to a particular range of the parameter  $n$ .

## 4. Space-time structure - Examples

### 4.1. a) $0 < n < 1$

In this case the range of variation of  $x$  is  $0 < x < +\infty$ . At the boundary of this interval  $h(0^+) \rightarrow -\infty$  and  $h(+\infty) \rightarrow 2(1-n)\lambda x$ .

From the expression for the curvature scalar  $R$  eq. (2.20) we see that  $x = 0$  represents a singularity as  $R \rightarrow +\infty$  there. On the other hand  $R(+\infty) \rightarrow 0$ , so  $x = +\infty$  represents the asymptotically flat region. There is one horizon, the event horizon, located at

$$x_0 = \left(\frac{\lambda}{M}\right)^{n-1} \frac{1}{2(1-n)\lambda}, \quad (4.1)$$

where  $h(x_0) = 0$ . This horizon divides the spacetime in a stationary region for  $x > x_0$  and an homogeneous one for  $x < x_0$ .

The fundamental building block is given in Fig. 1a. Note that the sector ending at the singularity  $x = 0$  is a triangle ( $f(0)$  is finite) and the singularity is spacelike. The complete Penrose diagram is shown in Fig. 1b.

Let us now consider the timelike geodesics equation in the Schwarzschild gauge (eq. (3.3))

$$\dot{x}^2 = E^2 - h(x) \quad (4.2)$$

where a dot indicates proper time differentiation. The qualitative behaviour of  $h(x)$  is shown in Fig. 1c. One notes that all geodesics fall into the singularity in a finite proper time

$$\tau = \int \frac{dx}{\sqrt{E^2 - h(x)}}. \quad (4.3)$$

The spacetime is therefore null and geodesically incomplete at  $x = 0$ .

Accelerated observers, moving on the trajectories  $x = \text{const.} > x_0$  see the geometry to be static and avoid to fall into the black hole. The acceleration vector of these observers is

$$a^\alpha = \left(0, \frac{h'(x)}{2}\right) \quad (4.4)$$

which is always directed to the right of the  $x$  axis.

Note that the  $(x, t)$  coordinates are not inertial at infinity. The metric there can be approximated by

$$ds^2 = -2(1-n)\lambda x dt^2 + \frac{dx^2}{2(1-n)\lambda x} \quad (4.5)$$

which has not the Minkowskian form.  $(x, t)$  are, in fact, Rindler coordinates associated to an acceleration  $(1-n)\lambda$ .

By the transformation

$$X = \sqrt{\frac{2x}{(1-n)\lambda}} \cosh(1-n)\lambda t, \quad T = \sqrt{\frac{2x}{(1-n)\lambda}} \sinh(1-n)\lambda t \quad (4.6)$$

the metric acquires the usual Minkowski form

$$ds^2 = -dT^2 + dX^2. \quad (4.7)$$

The interesting property of this spacetime is the fact that, due to the asymptotic behaviour of  $h(x) \sim 2(1-n)\lambda x$ , all geodesic observers get captured by the black hole. In fact, as one sees in Fig. 1c, outgoing (escaping) geodesics always reach a turning point and then fall back into the black hole. One can loosely think at this as a consequence of the black hole being accelerated to the right capturing all geodesic observers.

Finally we mention the behaviour of the coupling  $e^{\frac{2\phi}{n}}$ , which can be seen to vanish asymptotically (weak coupling region) and diverge on the singularity (strong coupling region).

#### 4.2. b) $1 < n < 2$

This case leads to a more complicated structure and contains two completely different subcases.

From the general expression eq. (2.15) we see that for  $1 < n < 2$   $x \in ]-\infty, 0]$ .

$h(x)$  vanishes at  $x = 0$  and so does  $R$ .  $x = 0$  corresponds, as we shall see, to an horizon, the acceleration horizon. On the other boundary  $R(-\infty) \rightarrow +\infty$ , so  $x = -\infty$  corresponds to a singularity of the spacetime.

Besides  $x = 0$ ,  $h(x)$  vanishes also at  $x = x_0$ , where  $x_0$  is given as before (see eq. (4.1)), but now  $x_0$  is negative.  $x = x_0$  is the location of the black hole horizon and there  $R(x_0) > 0$ . Finally  $h'(x)$  vanishes at

$$\tilde{x} = \left[ \frac{(n-1)\lambda}{nM} \right]^{n-1} \frac{1}{2(1-n)\lambda} \quad (4.8)$$

and the behaviour of  $h(x)$  is sketched in Fig. 2b.

From these considerations one deduces the basic building block which is represented in Fig. 2a.

Note that the end sector is triangular, since  $f(-\infty)$  is finite. The spacetime is null complete at the boundary  $x = -\infty$ , but it is timelike incomplete since the proper time  $\tau(-\infty)$  is finite.

Following similar arguments we find that the sector  $x_0 < x < 0$  is a square and that both timelike and null geodesics reach the boundary  $x = 0$  at a finite value of their affine parameters. The spacetime is regular at  $x = 0$ ; the metric there has the same behaviour as in eq. (4.5). Therefore  $x = 0$  represents an acceleration horizon with acceleration given as usual by its surface gravity  $(n-1)\lambda$ .

It seems then natural to look for analytical continuations of the the metric across this horizon for positive  $x$  values.

Of course, this doesn't mean that the solution is itself extensible through  $x = 0$ , since the dilaton field diverges there. However, we will relax any condition on  $\phi$  and see how the function in eq. (2.17) can be extended beyond its original domain.

Let us first discuss two smooth extensions which correspond to particular values of the parameter  $n$ :

- i)  $(-1)^{\frac{n}{n-1}} = 1$  even extension;
- ii)  $(-1)^{\frac{n}{n-1}} = -1$  odd extension.

In the case i) the metric for  $x > 0$  has the following  $h(x)$

$$h(x) = 2(1 - n)\lambda x - \frac{M}{\lambda} [2(n - 1)\lambda x]^{\frac{n}{n-1}}, \quad (4.9)$$

whereas for the case ii) we have

$$h(x) = 2(1 - n)\lambda x + \frac{M}{\lambda} [2(n - 1)\lambda x]^{\frac{n}{n-1}}. \quad (4.10)$$

We shall consider first the case i).

Being  $h(x)$  defined by eq. (4.9), we have that  $h(x)$  in the interval  $x \in [0, +\infty[$  vanishes only at  $x = 0$  and it is negative everywhere else (within this sector the spacetime is homogeneous).  $h'(x)$  is always negative and

$$R = -h''(x) = 4\lambda n M [2(n - 1)\lambda x]^{\frac{2-n}{n-1}}. \quad (4.11)$$

From this equation we see that  $x = +\infty$  corresponds to a singularity and, being  $f(+\infty)$  finite, the sector  $0 < x < +\infty$  is a triangle.

Adding together all information we can infer the behaviour of  $h(x)$  for  $x \in ]-\infty, +\infty[$  which is depicted in Fig. 3c. Also given are the building block and the complete Penrose diagram in Figs 3a and 3b.

We see that there are two horizons in the spacetime,  $x = x_0$  and  $x = 0$ . All timelike geodesics, but one, start and end at the spacelike singularities ( $x = \pm\infty$ ) reaching them in a finite proper time. The spacetime is timelike incomplete at the boundaries, but null complete.

The only geodesic which avoids falling into the singularity is  $x = \tilde{x}$ . Also accelerated observers  $x = \text{const.} = k$  ( $x_0 < k < 0$ ) escape the singularities. Their acceleration is directed to the right for  $x < \tilde{x}$  and to the left for  $\tilde{x} < x < 0$ .

$x = 0$  is the acceleration horizon for these comoving Rindler observers. Starting and end points of these trajectories (and of the  $x = \tilde{x}$  geodesic) are the dark dots in the Penrose diagram of Fig. 3b, which are the only points at infinity of this spacetime. No stationary motion is possible for  $x < x_0$  and  $x > 0$ .

The behaviour of the dilaton field for  $x > 0$  can be seen from (2.21) and (2.22). It is

$$e^{\frac{2}{n}\phi} = -[2(n-1)\lambda x]^{\frac{1}{n-1}}, \quad e^{-2\phi} = [2(n-1)\lambda x]^{\frac{n}{1-n}}. \quad (4.12)$$

Thus, while for  $x < 0$   $\phi$  is real and the two terms in (4.12) are positive, for  $x > 0$   $\phi$  becomes complex and acquires a constant imaginary part <sup>3</sup>

$$\phi \rightarrow \phi + i\frac{\pi n}{2(n-1)}. \quad (4.13)$$

This explains why  $e^{\frac{2}{n}\phi}$  becomes negative while  $e^{-2\phi}$  stays  $> 0$ . The coupling  $e^{\frac{2}{n}\phi}$  vanishes for  $x = 0$  and diverges on the singularity located at  $x = +\infty$ .

Now consider the case ii), with  $h(x)$  given by eq. (4.10).

$h(x)$  vanishes, for  $x \in [0, +\infty[$ , not only at  $x = 0$  but also at  $x = -x_0$ , which is the location of another horizon, the naked singularity horizon. The curvature scalar  $R$  vanishes at  $x = 0$  and is negative in the interval  $0 < x < +\infty$ . In particular  $R(+\infty) = -\infty$ , signalling the fact that  $x = +\infty$  is a singularity. Being  $h(x) > 0$  for  $x \rightarrow +\infty$  this singularity is timelike unlike the previous one.

Examination of  $f(x)$  reveals that the sector  $0 < x < -x_0$  is squared, but the last sector  $x > -x_0$  is a triangle. The corresponding building block is given in Fig. 4a, from which one deduces as resulting Penrose diagram of the maximal analytical extension of the spacetime a complicated network structure reproduced in Fig. 4b.

The spacetime is again null complete, but timelike incomplete at the boundaries  $x = \pm\infty$ . The graph reported in Fig. 4c shows the behaviour of  $h(x)$ ,  $x \in ]-\infty, +\infty[$ . We see that  $h(x)$  vanishes at three horizons,  $x = \pm x_0$  and  $x = 0$ .  $x = x_0$  is the black hole horizon,  $x = -x_0$  the naked singularity horizon and  $x = 0$  the acceleration horizon where the spacetime becomes flat (again in Rindler like coordinates).

The asymptotic behaviour of  $h(x)$  for  $x \rightarrow +\infty$  implies that no timelike geodesic reaches the timelike singularity. They all bounce back. There is bounded geodesic motion for  $x > \tilde{x}$ , with turning points at  $x > -x_0$ . All the other geodesics get eventually captured by the black hole singularity at  $x = -\infty$ . As before accelerated observers (and the  $x = \tilde{x}$  geodesic observer) avoid falling into the singularity and reach the asymptotic points of the diagram.

The acceleration of the  $x = \text{const.} = k$  ( $x_0 < k < 0$ ,  $k > -x_0$ ) observer is directed to the right for  $x < \tilde{x}$  and  $x > -x_0$  and to the left for  $\tilde{x} < x < 0$ .

Finally the dilaton, when  $x > 0$ , takes an imaginary part as in eq. (4.13), but now

$$e^{\frac{2}{n}\phi} = [2(n-1)\lambda x]^{\frac{1}{n-1}}, \quad e^{-2\phi} = -[2(n-1)\lambda x]^{\frac{n}{1-n}}. \quad (4.14)$$

---

<sup>3</sup> If one imposes a reality condition on  $\phi$  (see for example [7]) the surface  $x = 0$  must be considered a boundary of the spacetime, which is then timelike and null incomplete there.

For values of  $n$  different from the ones considered in the cases i) and ii) one can extend the metric to positive values of  $x$  introducing an absolute value, namely defining

$$h(x) = 2(1 - n)\lambda x - \frac{M}{\lambda} [2\lambda|x(1 - n)|]^{\frac{n}{n-1}}. \quad (4.15)$$

The resulting spacetime has a structure described by a Penrose diagram which is the same as the one given in Fig. 3b for the case i).

Alternatively, one could also consider

$$h(x) = 2(1 - n)\lambda x \left\{ 1 - \frac{M}{\lambda} [2\lambda|(1 - n)x|^{\frac{1}{n-1}}] \right\}. \quad (4.16)$$

The spacetime which results from this choice of  $h(x)$  is described by the Penrose diagram of Fig. 4b as for the case ii).

In these last two cases the coupling  $e^{\frac{2}{n}\phi}$  and the cosmological constant term  $e^{-2\phi}$  behave correspondingly as in i) and ii).

The same type of extensions have been considered in Ref [8] across the horizon of a semi-classical extremal black hole.

Note, finally, that due to the lack of a ‘true’ asymptotic region in the diagrams of Figs 3b and 4b,  $x = x_0$  cannot be considered an event horizon for our spacetimes.

### 4.3. c) $n = 2$

This case merits a discussion for himself because the resulting spacetime has constant curvature. In this case

$$h(x) = -2\lambda x - 4\lambda M x^2. \quad (4.17)$$

$h(x)$  vanishes for  $x = 0$  and  $x_0 = -\frac{1}{2M}$ .  $h'(x)$  vanishes at  $\tilde{x} = -\frac{1}{4M}$  and is positive for  $x < \tilde{x}$  and negative elsewhere. The behaviour of  $h(x)$  is depicted in Fig. 5c.

The extension of  $h(x)$  across  $x = 0$  is again considered without any requirement on  $\phi$ .

The scalar curvature  $R$  is a positive constant

$$R = 8\lambda M \quad (4.18)$$

and the spacetime is everywhere regular. The sectors  $-\infty < x < x_0$  and  $x > 0$  are triangular, whereas  $x_0 < x < 0$  is a square.

The fundamental building block and the Penrose diagram are depicted in Figs 5a and 5b.

The resulting spacetime is both null and timelike complete at the boundaries  $x = \pm\infty$ .

There are two horizons at  $x = 0$  and  $x = x_0$ . Accelerated observers at  $x = \text{const.} = k$  ( $x_0 < k < 0$ ) have their acceleration directed to the right for  $x < -\frac{1}{4M}$  and to the left for  $x > -\frac{1}{4M}$ . For  $x = -\frac{1}{4M}$  the trajectory is a geodesic. Typically geodesics run from one asymptotic region to the other or back.

A final comment concerns the dilaton field and the two terms

$$e^{\frac{2}{n}\phi} = e^\phi = -2\lambda x, \quad e^{-2\phi} = (-2\lambda x)^{-2}. \quad (4.19)$$

$\phi$  acquires, according to (4.13), an imaginary part  $+i\pi$ .  $x = 0$  is a weak-coupling region, while  $x = \pm\infty$  are strong-coupling.

#### 4.4. d) $n > 2$

Let us finally discuss briefly the case  $n > 2$ .

Being  $x < 0$ , we see that  $h(x)$  vanishes at  $x = 0$  and  $x = x_0$  ( $< 0$ ). The only horizon is at  $x = x_0$ . The null surface  $x = 0$  is a singularity because the curvature diverges there,  $R(0) \rightarrow +\infty$ .

The behaviour of  $h(x)$  is sketched in Fig. 6c. One deduces that the sector  $x_0 < x < 0$  is squared, whereas the sector  $x < x_0$  is triangular since  $f(-\infty)$  is finite.

The fundamental building block is depicted in Fig. 6a and the resulting Penrose diagram is given in Fig. 6b. Since null and timelike geodesics reach  $x = 0$  for finite values of their affine parameters, the spacetime is null and timelike incomplete at this boundary.

Stationary motion exists only for  $x > x_0$ .  $x = \text{const.} = k$  ( $x_0 < k$ ) observers have their acceleration directed to the right (increasing  $x$  values, towards the singularity) for  $x < \tilde{x}$  and to the left for  $x > \tilde{x}$ . Timelike geodesics coming from past infinity either have a turning point and continue to future infinity or proceed towards the singularity.

Note finally that the coupling  $e^{\frac{2}{n}\phi}$  vanishes on the singularity (which appears therefore in the weak coupling regime) and diverges asymptotically.

Although diverging at the singularity, the curvature  $R$  is integrable and the singularity is in some sense ‘mild’ as the tidal distortion remains finite when crossing the surface  $x = 0$ . One might extend the metric across  $x = 0$  and obtain a spacetime whose Penrose diagram is similar to the one obtained in the case  $n = 2$  (see Fig. 5b).

## 5. Conclusions

In this paper we have discussed the maximal extension of the space-times described by the solution of eqs (2.1) and (2.2).

In the case  $n = 1$  eq. (2.11) reduces to the usual black hole solution of Ref [3], for which there exists an asymptotic minkowskian and static frame. This is not true anymore for  $n \neq 1$  and this simple fact gives the interesting implications that emerged in section 4, which we here summarize.

For  $0 < n < 1$ , as for  $n = 1$ , the Penrose diagram is the same as that of a Schwarzschild black hole. However, the static frame  $(x, t)$  of eq. (3.3) is not asymptotically minkowskian, but Rindler like (see eq. (4.5)). One can introduce the inertial frame  $(X, T)$ , defined in (4.6), but as a result the metric is nonstatic.

As a consequence of the fact that the black hole can be thought to be accelerated, all geodesic observers get soon or later captured and inevitably end their journey into the singularity. The only way to avoid this fate and reach safely the asymptotic region along a timelike trajectory is to have a nonzero acceleration, as for instance the curves  $x = \text{const.}$

For values of  $n$  such that  $1 < n < 2$  a completely different causal structure emerges, as it is shown in Figs 3b and 4b.

Fig. 3b suggests the existence of two black holes, one at each end of the  $x$  axis. They are both attracting and the combined action of their gravitational fields pulls any observer at  $x < \tilde{x}$  (see eq. (4.8)) towards the black hole located at  $x = -\infty$  and those at  $x > \tilde{x}$  towards the other one. At  $x = \tilde{x}$ , although the scalar curvature  $R$  doesn't vanish, there is an equilibrium between the two forces.

$R$  vanishes at  $x = 0$ , the location of the acceleration horizon for Rindler observers. Inertial observers, on the other hand, can cross this horizon and enter a collapsing cosmological region defined for  $x > 0$ , as in the case of a black hole immersed in a closed universe.

The diagram of Fig. 4b has qualitatively a similar description till  $x = 0$ , but now the gravitational collapse of the  $x > 0$  region is not strong enough to cause the 'big crunch' singularity. Rather a wormhole appears, through which one can safely travel to a new universe similar to the one just left. This multi-black hole structure possesses both spacelike and timelike singularities, all strong-coupling in the dilaton field.

In the case  $n = 2$  the structure of the Penrose diagram of Fig. 5b is similar to that of Fig. 3b except for the important fact that the singularities are replaced by asymptotic well-behaved regions of the two-dimensional metric.

Finally, for  $n > 2$  the form of the diagram is the same as in Fig. 1b, but with the singularity and the asymptotic regions exchanged: the singularity is now light-like.

The spacetime features we have explored here are not peculiar of our two-dimensional theory eq. (1.1). They appear also in the context of higher-derivative  $2d$  gravity, as for example in [9].

Let us consider the action

$$S = \int d^2x \sqrt{-g} \left[ \frac{R^{k+1}}{16} + \Lambda \right], \quad (5.1)$$

where  $k$  is a positive integer. The trace and the traceless part of the field equations are

$$\frac{k}{16} R^{k+1} + \frac{(k+1)}{16} \nabla^2 R^k = \Lambda, \quad \nabla_\mu \partial_\nu R^k - \frac{1}{2} g_{\mu\nu} \nabla^2 R^k = 0. \quad (5.2)$$

In the Schwarzschild gauge eq. (3.3), where  $R = -h''(x)$ , eqs (5.2) give the third-order equation

$$\frac{k(k+1)}{16} h'''(x) h'(x) + \Lambda [-h''(x)]^{1-k} = \frac{k[h''(x)]^2}{16}. \quad (5.3)$$

The general solution of eq. (5.3) is

$$h(x) = C + B\Lambda x + Dx^{2+\frac{1}{k}}, \quad (5.4)$$

where

$$B = -\frac{-16[-D(2+\frac{1}{k})(1+\frac{1}{k})]^{1-k}}{k(1+\frac{1}{k})^2(2+\frac{1}{k})D}. \quad (5.5)$$

The scalar curvature of these solutions is

$$R = -(2 + \frac{1}{k})(1 + \frac{1}{k})Dx^{\frac{1}{k}}. \quad (5.6)$$

Note that for  $C = 0$   $h(x)$  has the same structure of our eq. (2.17) with  $k = \frac{n-1}{2-n}$ .

One can proceed with the analysis of the spacetime structure of these solutions along the line of the previous paragraph. Here we just mention that for  $k = 1$ ,  $C = 0$  and  $D = \frac{2}{3}$ , as considered in Ref [6], the function  $h(x)$  has the same behaviour of eq. (2.17) with  $n = \frac{3}{2}$  and the resulting Penrose diagram is represented in Fig. 4b.

*Note added:* After completion of this work we learnt that the spacetime structure of our model has been briefly discussed in a recent preprint by M.O. Katanaev, W. Kummer and H. Liebl, *On the Completeness of the Black Hole Singularity in 2d Dilaton Theories*, gr-qc/9602040. These authors seem, however, not to have paid much attention to our model because of “problems of interpretation” related to the asymptotic Rindler structure of the spacetime.

Acknowledgements: We would like to thank D. Amati and J.G. Russo for useful discussions.

## References

- [1] J.G. Russo, L. Susskind and L. Thorlacius, Phys. Rev. D46 (1992) 3444; Phys. Rev. D47 (1993) 533.
- [2] A. Fabbri and J.G. Russo, *Soluble models in 2d dilaton gravity*, hep-th/9510109 (to appear in Phys. Rev. D).
- [3] C. Callan, S. Giddings, J. Harvey and A. Strominger, Phys. Rev. D45 (1992) R1005.
- [4] J.D. Brown, M. Henneaux and C. Teitelboim, Phys. Rev. D33 (1986), 319; R.B. Mann, Gen. Rel. Grav. 24 (1992), 433.
- [5] J.S. Lemos and P.M. Sa, Phys. Rev. D49 (1994) 2897; M.O. Katanaev, W. Kummer and H. Liebl, *Geometric interpretation and classification of global solutions in generalized dilaton gravity*, gr-qc/9511009.
- [6] T. Klösch and T. Strobl, *Classical and Quantum Gravity in 1+1 dimensions Part I: A unifying approach*, gr-qc/9508020; *Classical and Quantum Gravity in 1+1 dimensions Part II: The universal coverings*, gr-qc/9511081.
- [7] M. Cadoni and S. Mignemi, *On the conformal equivalence between 2d black holes and Rindler spacetime*, gr-qc/9505032.
- [8] S.P. Trivedi, Phys. Rev. D47 (1993) 4233.
- [9] H.J. Schmidt, J. Math. Phys. 32 (1991) 1562; S. Mignemi and H.J. Schmidt, Class. Quant. Grav. 12 (1995) 849.

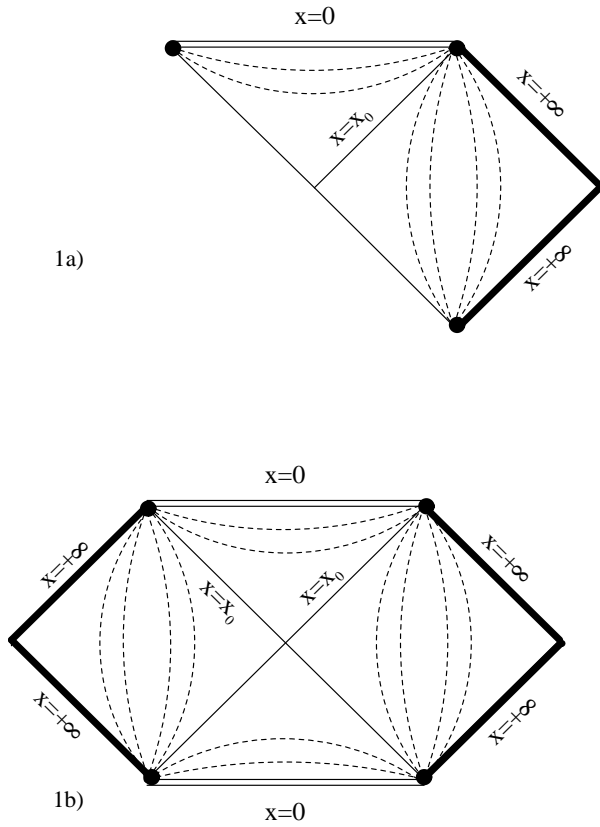


**Fig. 1:** Fundamental building block in a) and Penrose diagram in b) for the case  $0 < n < 1$ . Double lines represent the singularity, dashed lines the curves  $x = \text{const.}$ , regular lines the horizons and thick lines the asymptotic region.

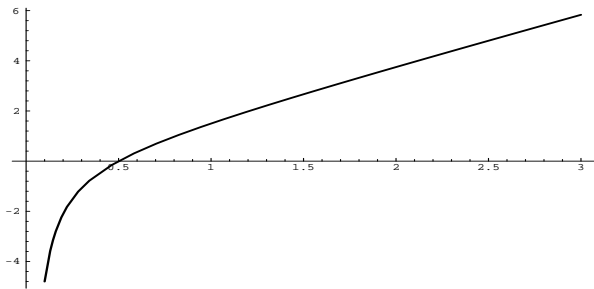


**Fig. 1c:** Graph of  $h(x)$  for  $0 < n < 1$  (here  $\lambda = M = \frac{1}{n-1}$ ).

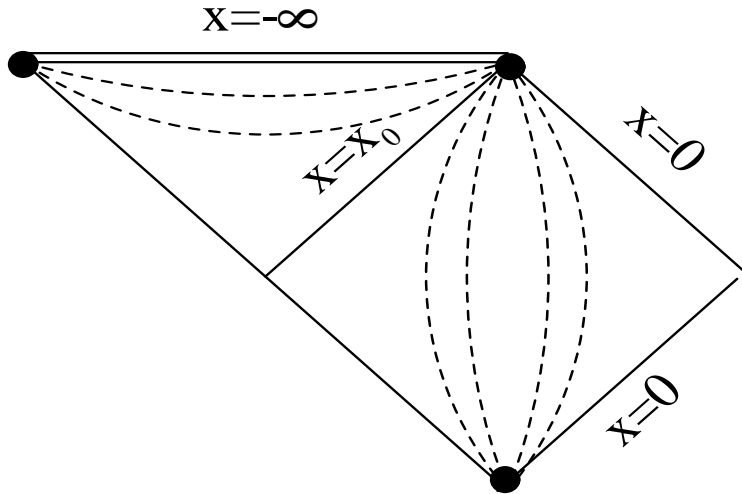


**Fig. 2a:** Building block for the case  $1 < n < 2$  till  $x = 0$ .

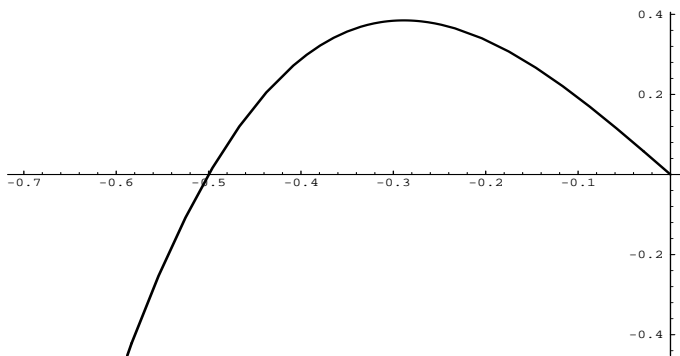


**Fig. 2b:** Graph of  $h(x)$  for the case in Fig. 2a.

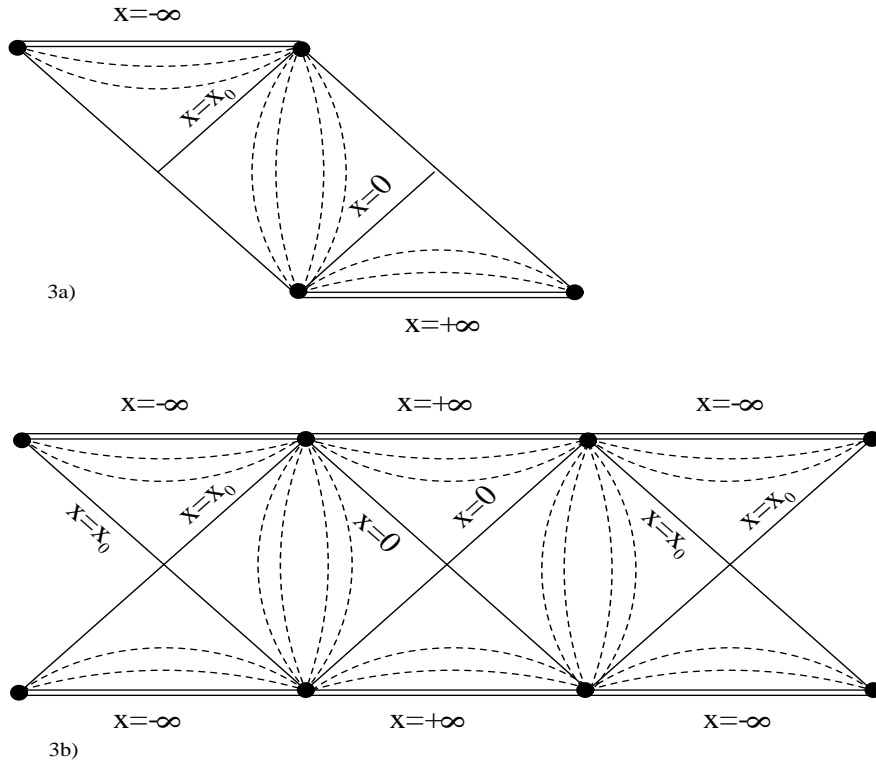


**Fig. 3:** Fundamental building block in a) and Penrose diagram in b) for the extension i).

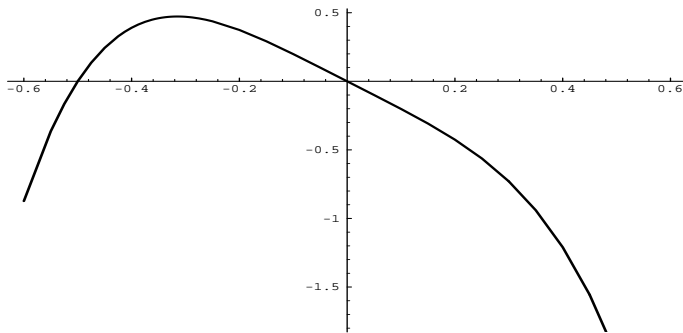
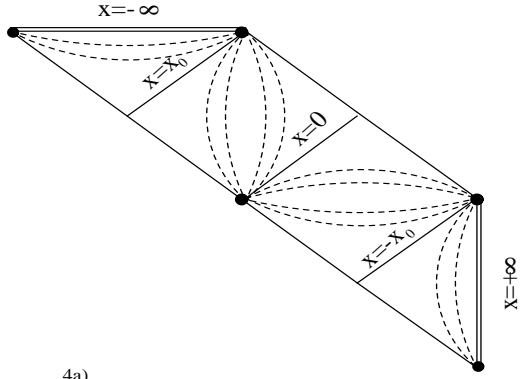
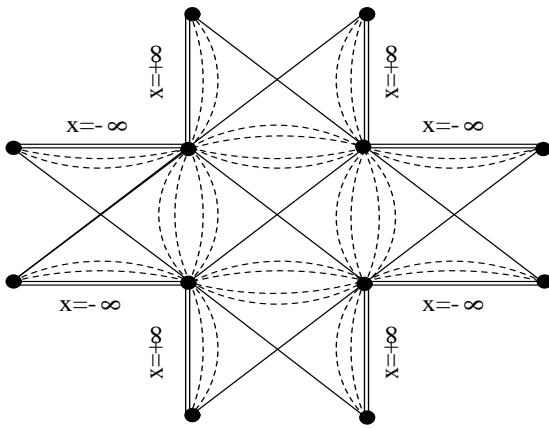


**Fig. 3c:** Graph of  $h(x)$  in the case i).



4a)



4b)

**Fig. 4:** Fundamental building block in a) and Penrose diagram in b) for the extension ii).

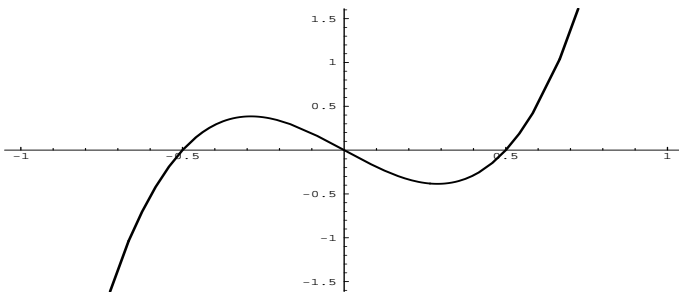


**Fig. 4c:** Graph of  $h(x)$  in the case ii).

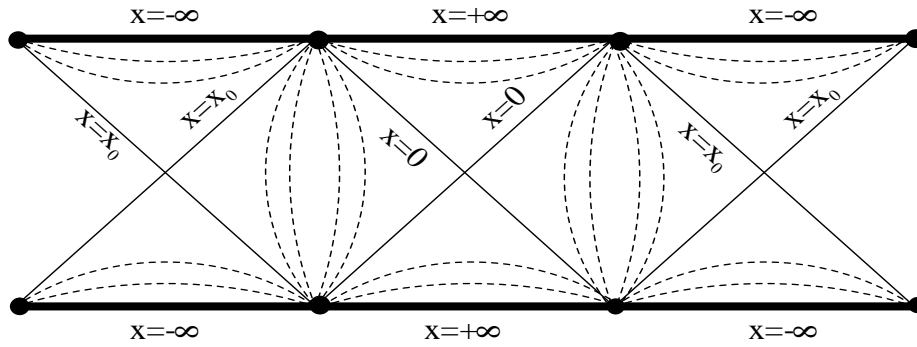
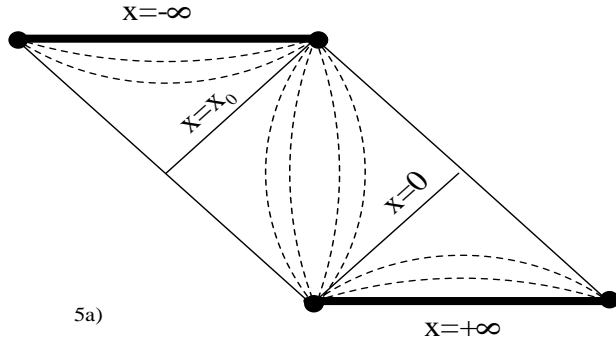


**Fig. 5:** Fundamental building block in a) and Penrose diagram in b) in the case  $n = 2$ .

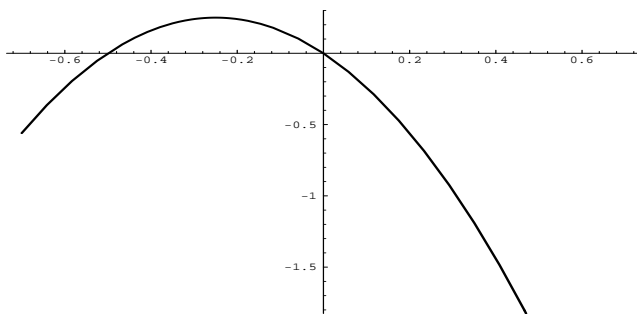


**Fig. 5c:** Graph of  $h(x)$  for  $n = 2$ .

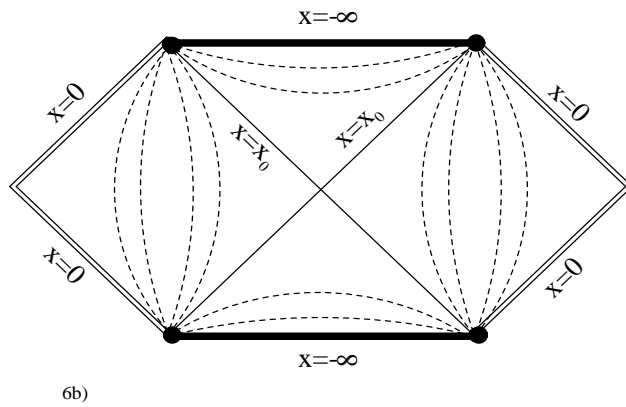
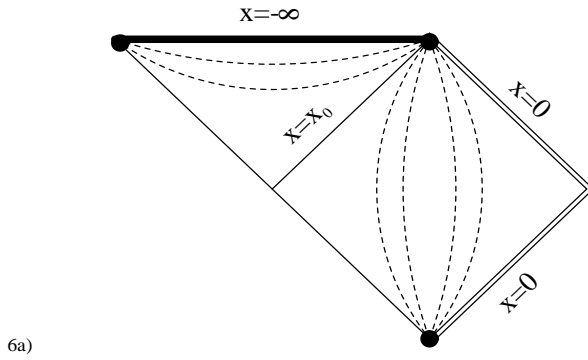


**Fig. 6:** Fundamental building block in a) and Penrose diagram in b) in the case  $n > 2$ .

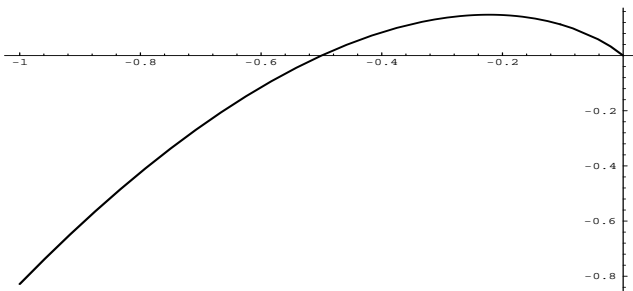


**Fig. 6c:** Graph of  $h(x)$  for  $n > 2$ .